Inorganic Chemistry
Article

Inorg. Chem. **2010**, *49*, 2047–2056 **2047**
DOI: 10.1021/ic901600v

Bimetallic Materials Derived from Manganese(III) Schiff Base Complexes and Pentacyanidonitrosylferrate(II) Precursor: Structures and Magnetic Properties

Chun Yang,[†,§] Qing-Lun Wang,*[,†] Yue Ma,[†] Guo-Tao Tang,[†] Dai-Zheng Liao,*[,‡] Shi-Ping Yan,[†] Guang-Ming Yang,[†] and Peng Cheng[†]

[†]*Department of Chemistry, Nankai University, Tianjin, 300071, P. R. China,* [‡]*Key Laboratory of Metal and Molecular Material Chemistry of Tianjin City, Nankai University, Tianjin, 300071, P. R. China, and* [§]*School of Chemical Engineering and Technology, Hebei University of Technology, Tianjin, 300130, P. R. China*

Received August 11, 2009

Three complexes, $[Mn(salphen)(H_2O)]_2[Fe(CN)_5(NO)]\cdot 2CH_3OH$ (**1**) (salphen = *N*,*N*′-phenylenebis(salicylideneiminato) dianion), $[Mn(naphtmen)(CH_3OH)]_2[Fe(CN)_5(NO)]$ (**2**) (naphtmen = *N*,*N*′-(1,1,2,2-tetramethylethylene)-bis(naphthylideneiminato) dianion), and $\{[Mn(salen)]_2[Fe(CN)_5(NO)]\cdot H_2O\}_n$ (**3**) (salen = *N*,*N*′-ethylene-bis-(salicylideneiminato) dianion), were synthesized and structurally characterized by X-ray single-crystal diffraction. The structural analyses show that complexes **1** and **2** consist of the discrete linear trinuclear $[Mn(SB)]_2[Fe(CN)_5(NO)]$ units (SB = salphen for **1**, naphtmen for **2**); in complex **3**, the nitroprusside anion coordinates to the axial sites of the four $[Mn(salen)]^+$ entities through its four cyano nitrogen atoms, providing a two-dimensional network. The magnetic analysis indicates that the nitroprusside bridging ligand propagates a very weak antiferromagnetic exchange and single-ion anisotropy (*D*) plays an important role in the overall magnetic properties. Different from complexes **2** and **3**, complex **1** shows a typical spin-flop transition with a critical field of 20 kOe.

Introduction

Molecular magnetism is of considerable interest both for designing new magnetic materials with potential usage in information storage and for investigating the relationship between the structure and magnetic behavior.[1] Recent studies include bulk materials with spontaneous magnetization at high T_C values even above room temperature,[2] hybrid magnetic compounds with dual properties exemplified as magneto-chiral dichroism,[3] photomagnetic effects,[4] metal-organic multiferroics,[5] and porous magnetic metal−organic frameworks,[6] as well as molecular nanomagnets such as single-molecule magnets (SMMs)[7] or single-chain magnets (SCMs)[8] exhibiting a slow relaxation of magnetization. Some interesting phenomena in magnetism are also found in antiferromagnetically coupled compounds, such as spin-canting, metamagnetic transition, spin-flop transition, and so forth,[9−15] which are simply sketched in Scheme 1.[15e] Spin-canting means the noncollinear spin arrangements on two sublattices of an

*To whom correspondence should be addressed. E-mail: wangql@nankai.edu.cn (Q.-L.W.); liaodz@nankai.edu.cn (D.-Z.L.).

(1) (a) Kröber, J.; Codjovi, E.; Kahn, O.; Grolière, F.; Jay, C. *J. Am. Chem. Soc.* **1993**, *115*, 9810. (b) Kahn, O. *Molecular Magnetism*; VCH Publishers: New York, 1993. (c) Gatteschi, D.; Sessoli R.; Villain, J. *Molecular Nanomagnets*, Oxford University Press: Oxford, U. K., 2006.

(2) (a) Manriquez, J. M.; Yee, G. T.; McLean, R. S.; Epstein, A. J.; Miller, J. S. *Science* **1991**, *252*, 1415. (b) Holmes, S. M.; Girolami, G. S. *J. Am. Chem. Soc.* **1999**, *121*, 5593.

(3) (a) Imai, H.; Inoue, K.; Kikuchi, K.; Yoshida, Y.; Ito, M.; Sunahara, T.; Onaka, S. *Angew. Chem., Int. Ed.* **2004**, *43*, 5618. (b) Inoue, K.; Imai, H.; Ghalsasi, P. S.; Kikuchi, K.; Ohba, M.; Ōkawa, H.; Yakhmi, J. V. *Angew. Chem., Int. Ed.* **2001**, *40*, 4242.

(4) (a) Sato, O.; Iyoda, T.; Fujishima, A.; Hashimoto, K. *Science* **1996**, *272*, 704. (b) Hozumi, T.; Hashimoto, K.; Ohkoshi, S. *J. Am. Chem. Soc.* **2005**, *127*, 3864. (c) Ohkoshi, S.; Ikeda, S.; Hozumi, T.; Kashiwagi, T; Hashimoto, K. *J. Am. Chem. Soc.* **2006**, *128*, 5320. (d) Herrera, J. M.; Marvaud, V.; Verdaguer, M.; Marrot, J.; Kalisz, M.; Mathonière, C. *Angew. Chem., Int. Ed.* **2004**, *43*, 5468.

(5) (a) Cui, H. B.; Wang, Z.; Takahashi, K.; Okano, Y.; Kobayashi, H.; Kobayashi, A. *J. Am. Chem. Soc.* **2006**, *128*, 15074. (b) Ohkoshi, S.; Tokoro, H.; Matsuda, T.; Takahashi, H.; Irie, H.; Hashimoto, K. *Angew. Chem., Int. Ed.* **2007**, *46*, 3238. (c) Jain, P.; Dalal, N. S.; Toby, B. H.; Kroto, H. W.; Cheetham, A. K. *J. Am. Chem. Soc.* **2008**, *130*, 10450.

(6) (a) Kaye, S. S.; Long, J. R. *J. Am. Chem. Soc.* **2005**, *127*, 6506. (b) Beauvais, L. G.; Long, J. R. *J. Am. Chem. Soc.* **2002**, *124*, 12096.

(7) (a) Gatteschi, D.; Sessoli, R. *Angew. Chem., Int. Ed.* **2003**, *42*, 268−297 and references therein. (b) Beltran, L. M. C.; Long, J. R. *Acc. Chem. Res.* **2005**, *38*, 325−334 and references therein. (c) del Barco, E.; Kent, A. D.; Hill, S.; North, J. M.; Dalal, N. S.; Rumberger, E. M.; Hendrickson, D. N.; Chakov, N.; Christou, G. *J. Low Temp. Phys.* **2005**, *140*, 119.

(8) For examples, see: (a) Caneschi, A.; Gatteschi, D.; Lalioti, N.; Sangregorio, C.; Sessoli, R.; Venturi, G.; Vindigni, A.; Rettori, A.; Pini, M. G.; Novak, M. A. *Angew. Chem., Int. Ed.* **2001**, *40*, 1760. (b) Lescouëzec, R.; Vaissermann, J.; Ruiz-Pérez, C.; Lloret, F.; Carrasco, R.; Julve, M.; Verdaguer, M.; Dromzee, Y.; Gatteschi, D.; Wernsdorfer, W. *Angew. Chem., Int. Ed.* **2003**, *42*, 1483. (c) Liu, T. F.; Fu, D.; Gao, S.; Zhang, Y. Z.; Sun, H. L.; Su, G.; Liu, Y. J. *J. Am. Chem. Soc.* **2003**, *125*, 13976. (d) Toma, L. M.; Lescouëzec, R.; Pasán, J.; Ruiz-Pérez, C.; Vaissermann, J.; Cano, J.; Carrasco, R.; Wernsdorfer, W.; Lloret, F.; Julve, M. *J. Am. Chem. Soc.* **2006**, *128*, 4842. (e) Miyasaka, H.; Julve, M.; Yamashita, M.; Clérac, R. *Inorg. Chem.* **2009**, *48*, 3420.

(9) (a) Carlin, R. L.; Van-Duyneveldt, A. J. *Magnetic Properties of Transition Metal Compounds*; Springer-Verlag: New York, 1977. (b) Carlin, R. L. *Magnetochemistry*; Springer-Verlag: Berlin, 1986.

Published on Web 01/12/2010

Scheme 1. Sketches of the Spin-Canting, Metamagnetism, and Spin-Flop Phenomena

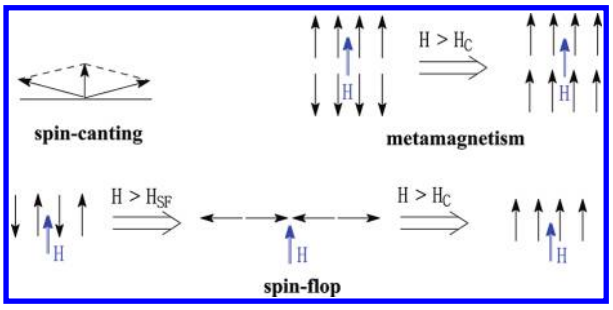

antiferromagnet.[9−12] The metamagnet is the one with net moments aligned antiparallelly by weak antiferromagnetic (AF) interactions, which are of secondary importance. A large external field could overwhelm the weak AF interactions and turn the system to a ferro-, ferri-, or weak-ferromagnetic state, depending on the details of the spin alignments in the AF state.[9,12,13] When a spin-flop happens, a field parallel to the easy axis of an antiferromagnet causes the spins to first flop to the direction perpendicular to it and then parallel to the easy axis until another critical field (H_C) is reached.[9,11,14,15] Although these three phenomena are different in many aspects, there also exist some common features, such as the important role of the magnetic anisotropy in all of them. Generally, a large anisotropy leads to a significant spin-canting through increasing the possible antisymmetric super-exchange interaction and may induce a metamagnetic transition in the presence of competing interactions, while a small anisotropy favors the spin-flop transition.[9,14,15]

The Mn(III) ions in Mn Schiff base complexes mainly within N_2O_2 basal environments have strong uniaxial magnetic anisotropy created by crystal fields of different ligands in six-coordinated surroundings together with the Jahn−Teller effect. The $[Mn(SB)]^+$ (where SB = Schiff base) cations whose apical sites can be filled by incoming bridges or their phenoxides have been utilized as useful tectons for the construction of coordination compounds with desirable properties. Self-assemblies of $[Mn(SB)]^+$ and hexacyanometalates $[M(CN)_6]^{3-}$ (M = Fe(III), Cr(III)) or octacyanometalates $[M(CN)_8]^{n-}$ (M = Mo(IV), Mo(V), W(IV), W(V)) showed a rich variety of structures ranging from clusters[16,17] and one-dimensional chains[18,19] to two-dimensional sheets.[20] There are also reports of complete coordinated three-dimensional networks based on polycyano polymetal clusters such as $[Re_6Se_8(CN)_6]^{4-}$ and $[Nb_6Cl_{12}(CN)_6]^{4-}$.[21] Some of them exhibit SMM[16,22] or SCM[18,23] properties induced by anisotropic sources of Mn(III) and Fe(III). Furthermore, polynuclear[24] or one-dimensional chains[25] formed by $[Mn(SB)]^+$ and tetracyano-bearing precursors $[Cr(L)(CN)_4]^-$ (L = 2,2′-bipyrimidine, 2,2′-bipy or 9,10-phen) were also synthesized successfully. However, the combination of $[Mn(SB)]^+$ and pentacyanometalate, for instance, $[Fe(CN)_5(NO)]^{2-}$ and $[Cr(CN)_5(NO)]^{3-}$, was rarely reported.[26] In this paper, two trinuclear complexes, $[Mn(salphen)(H_2O)]_2[Fe(CN)_5(NO)]\cdot 2CH_3OH$ (**1**) (salphen = *N*,*N*′-phenylenebis(salicylideneiminato) dianion) and $[Mn(naphtmen)(CH_3OH)]_2[Fe(CN)_5(NO)]$ (**2**) (naphtmen = *N*,*N*′-(1,1,2,2-tetramethylethylene)bis(naphthylideneiminato) dianion), and a two-dimensional complex, $\{[Mn(salen)]_2[Fe(CN)_5(NO)]\cdot H_2O\}_n$ (**3**) (salen = *N*,*N*′-ethylene-bis(salicylideneiminato) dianion), derived from manganese(III) Schiff base complexes and a pentacyanidonitrosylferrate(II) precursor have been synthesized.

(10) For examples, see: (a) Rettig, S. J.; Storr, A.; Summers, D. A.; Thompson, R. C.; Trotter, J. *J. Am. Chem. Soc.* **1997**, *119*, 8675. (b) Batten, S. R.; Jensen, P.; Kepert, C. J.; Kurmoo, M.; Moubaraki, B.; Murray, K. S.; Price, D. J. *J. Chem. Soc., Dalton Trans.* **1999**, 2987. (c) Richard-Plouet, M.; Vilminot, S.; Guillot, M.; Kurmoo, M. *Chem. Mater.* **2002**, *14*, 3829. (d) Wang, X. Y.; Gan, L.; Zhang, S. W.; Gao, S. *Inorg. Chem.* **2004**, *43*, 4615. (e) Salah, M. B.; Vilminot, S.; André, G.; Bourée-Vigneron, F.; Richard-Plouet, M.; Mhiri, T.; Kurmoo, M. *Chem. Mater.* **2005**, *17*, 2612.

(11) (a) Zora, J. A.; Seddon, K. R.; Hitchcock, P. B.; Lowe, C. B.; Shum, D. P.; Carlin, R. L. *Inorg. Chem.* **1990**, *29*, 3302. (b) Schlueter, J. A.; Manson, J. L.; Hyzer, K. A.; Geiser, U. *Inorg. Chem.* **2004**, *43*, 4100.

(12) (a) Gao, E. Q.; Wang, Z. M.; Yan, C. H. *Chem. Commun.* **2003**, 1748. (b) Zeng, M. H.; Zhang, W. X.; Sun, X. Z.; Chen, X. M. *Angew. Chem., Int. Ed.* **2005**, *44*, 3079.

(13) For examples, see: (a) Kou, H. Z.; Gao, S.; Sun, B. W.; Zhang, J. *Chem. Mater.* **2001**, *13*, 1431. (b) Gao, E. Q.; Yue, Y. F.; Bai, S. Q.; He, Z.; Yan, C. H. *J. Am. Chem. Soc.* **2004**, *126*, 1419. (c) Pereira, C. L. M.; Pedroso, E. F.; Stumpf, H. O.; Novak, M. A.; Ricard, L.; Ruiz-García, R.; Rivière, E.; Journaux, Y. *Angew. Chem., Int. Ed.* **2004**, *43*, 955. (d) Toma, L.; Lescoëzec, R.; Vaissermann, J.; Delgado, F. S.; Ruiz-Pérez, C.; Carrasco, R.; Cano, J.; Lloret, F.; Julve, M. *Chem.—Eur. J.* **2004**, *10*, 6130. (e) Zhang, Y. Z.; Gao, S.; Sun, H. L.; Su, G.; Wang, Z. M.; Zhang, S. W. *Chem. Commun.* **2004**, 1906.

(14) Carlin, R. L.; van Duyneveldt, A. J. *Acc. Chem. Res.* **1980**, *13*, 231.

(15) For examples, see: (a) Manson, J. L.; Huang, Q. Z.; Lynn, J. W.; Koo, H. J.; Whangbo, M. H.; Bateman, R.; Otsuka, T.; Wada, N.; Argylou, D. N.; Miller, J. S. *J. Am. Chem. Soc.* **2001**, *123*, 162. (b) Ma, B. Q.; Sun, H. L.; Gao, S.; Su, G *Chem. Mater.* **2001**, *13*, 1946. (c) Salah, M. B.; Vilminot, S.; André, G.; Richard-Plouet, M.; Bourée-Vigneron, F.; Mhiri, T.; Kurmoo, M. *Chem.—Eur. J.* **2004**, *10*, 2048. (d) Sun, H. L.; Gao, S.; Ma, B. Q.; Su, G.; Batten, S. R. *Cryst. Growth Des.* **2005**, *5*, 269. (e) Wang, X. Y.; Wang, L.; Wang, Z. M.; Su, G.; Gao, S. *Chem. Mater.* **2005**, *17*, 6369.

(16) Choi, H. J.; Sokol, J. J.; Long, J. R. *Inorg. Chem.* **2004**, *43*, 1606.

(17) For examples, see: (a) Miyasaka, H.; Matsumoto, N.; Ōkawa, H.; Re, N.; Gallo, E.; Floriani, C. *J. Am. Chem. Soc.* **1996**, *118*, 981. (b) Miyasaka, H.; Ieda, H.; Matsumoto, N.; Re, N.; Crescenzi, R.; Floriani, C. *Inorg. Chem.* **1998**, *37*, 255. (c) Ko, H. H.; Lim, J. H.; Yoo, H. S.; Kang, J. S; Kim, H. C.; Koh, E. K.; Hong, C. S. *Dalton Trans.* **2007**, 2070. (d) Przychodzeń, P.; Lewiński, K.; Balanda, M.; Pelka, R.; Rams, M.; Wasiutyński, T.; Guyard-Duhayon, C.; Sieklucka, B. *Inorg. Chem.* **2004**, *43*, 2967. (e) Przychodzeń, P.; Rams, M; Guyard-Duhayon, C; Sieklucka, B. *Inorg. Chem. Commun.* **2005**, *8*, 350.

(18) Ferbinteanu, M.; Miyasaka, H.; Wernsdorfer, W.; Nakata, K.; Sugiura, K.; Yamashita, M.; Coulon, C.; Clérac, R. *J. Am. Chem. Soc.* **2005**, *127*, 3090.

(19) (a) Re, N.; Gallo, E.; Floriani, C.; Miyasaka, H.; Matsumoto, N. *Inorg. Chem.* **1996**, *35*, 6004. (b) Yoo, H. S.; Ko, H. H.; Ryu, D. W.; Lee, J. W.; Yoon, J. H.; Lee, W. R.; Kim, H. C.; Koh, E. K.; Hong, C. S. *Inorg. Chem.* **2009**, *48*, 5617.

(20) (a) Miyasaka, H.; Okawa, H.; Miyazaki, A.; Enoki, T. *Inorg. Chem.* **1998**, *37*, 4878. (b) Kou, H. Z.; Ni, Z. H.; Zhou, B. C.; Wang, R. J. *Inorg. Chem. Commun.* **2004**, *7*, 1150.

(21) (a) Kim, Y.; Park, S. M.; Kim, S. J. *Inorg. Chem. Commun.* **2002**, *5*, 592. (b) Zhang, J. J.; Lachgar, A. *J. Am. Chem. Soc.* **2007**, *129*, 250.

(22) (a) Miyasaka, H.; Clérac, R.; Wernsdorfer, W.; Lecren, L.; Bonhomme, C.; Sugiura, K.; Yamashita, M. *Angew. Chem., Int. Ed.* **2004**, *43*, 2801. (b) Lu, Z. L.; Yuan, M.; Pan, F.; Gao, S.; Zhang, D. Q.; Zhu, D. B. *Inorg. Chem.* **2006**, *45*, 3538. (c) Kachi-Terajima, C.; Miyasaka, H.; Sugiura, K.; Clérac, R.; Nojiri, H. *Inorg. Chem.* **2006**, *45*, 4381.

(23) (a) Miyasaka, H.; Clérac, R. *Bull. Chem. Soc. Jpn.* **2005**, *78*, 1725. (b) Clérac, R.; Miyasaka, H.; Yamashita, M.; Coulon, C. *J. Am. Chem. Soc.* **2002**, *124*, 12837. (c) Miyasaka, H.; Madanbashi, T.; Sugimoto, K.; Nakazawa, Y.; Wernsdorfer, W.; Sugiura, K.; Yamashita, M.; Coulon, C.; Clérac, R. *Chem.—Eur. J.* **2006**, *12*, 7028.

(24) Visinescu, D.; Toma, L. M.; Lloret, F.; Fabelo, O.; Ruiz-Pérezc, C.; Julve, M. *Dalton Trans.* **2009**, 37.

(25) (a) Pan, F.; Wang, Z.-M.; Gao, S. *Inorg. Chem.* **2007**, *46*, 10221. (b) Visinescu, D.; Toma, L. M.; Lloret, F.; Fabelo, O.; Ruiz-Pérezc, C.; Julve, M. *Dalton Trans.* **2008**, 4103.

(26) (a) Clemente-León, M.; Coronado, E.; Galán-Mascarós, J. R.; Gómez-García, C. J.; Woike, T.; Clemente-Juan, J. M. *Inorg. Chem.* **2001**, *40*, 87. (b) Ababei, R.; Li, Y. G.; Roubeau, O.; Kalisz, M.; Bréfuel, N.; Coulon, C.; Harté, E.; Liu, X.; Mathonière, C.; Clérac, R. *New J. Chem.* **2009**, *33*, 1237. (c) Ni, Z. H.; Zheng, L.; Zhang, L. F.; Cui, A. L.; Ni, W. W.; Zhao, C. C.; Kou, H. Z. *Eur. J. Inorg. Chem.* **2007**, 1240. (d) Shaikh, N.; Panja, A.; Goswami, S.; Banerjee, P.; Kubiak, M.; Ciunik, Z.; Puchalska, M.; Legendziewicz, J. *Indian J. Chem. A* **2004**, *43A*, 1403.

Scheme 2. Schiff Base Ligands of the Mn(III) Complex Precursors

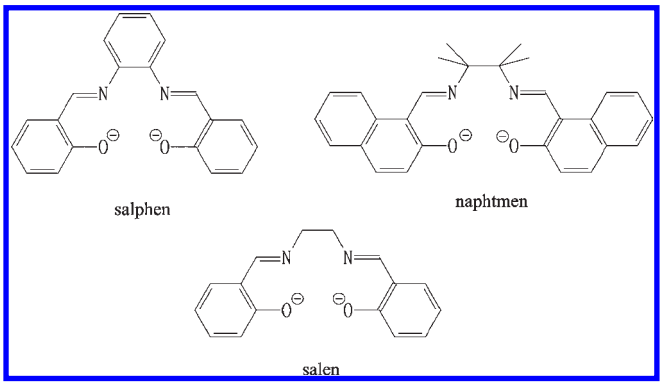

The crystal structures, spectroscopy, and magnetic properties of these complexes were also investigated.

Experimental Section

General. All of the reagents were commercially available and used without further purification. The quadridentate Schiff base ligands H_2salphen, H_2naphtmen, and H_2salen were prepared by mixing salicylaldehyde or naphthylaldehyde and the corresponding diamine in a 2:1 molar ratio in ethanol, according to the literature (Scheme 2).[27] The C, H, and N elemental analyses were carried out with a Perkin−Elmer 240C elemental analyzer. The IR spectra were recorded as KBr pellets on a Bruker Tensor 27 FTIR spectrophotometer in the 4000−400 cm^{-1} regions. Magnetic susceptibilities were measured on a Quantum Design MPMS-7 SQUID magnetometer. Diamagnetic corrections were made with Pascal's constants for all of the constituent atoms.[28] The heat capacity was measured at zero applied field by a relaxation method using a commercial Physical Property Measurement System (PPMS-9, Quantum Design).

Preparation of [Mn(SB)(H_2O)]ClO_4 (SB = salphen, naphtmen, or salen for 1, 2, or 3, respectively). The manganese(III) precursors were prepared by mixing $Mn(OAc)_3\cdot 2H_2O$, H_2SB, and $NaClO_4$ in methanol/H_2O with a molar ratio of 1:1:1.5, according to the method reported previously.[17d,29]

Preparation of Complex 1. To a reddish brown solution of [Mn(salphen)(H_2O)]ClO_4 (0.0973 g, 0.2 mmol) in methanol (30 mL) was added dropwise a solution of $Na_2[Fe(CN)_5NO]\cdot 2H_2O$ (0.0298 g, 0.1 mmol) in water (5 mL). The dark brown solution was stirred for 30 min and then filtered. The dark brown filtrate was left undisturbed in the air at room temperature, and well-formed black single crystals of complex **1** suitable for X-ray structure analysis were obtained from the mother liquor by slow evaporation for one week or so. The crystals were collected by suction filtration, washed with the minimum volume of ice cold water, and dried in the air. Anal. Calcd for $C_{47}H_{40}FeMn_2N_{10}O_9$(1054.62): C, 53.53; H, 3.82; N, 13.28%. Found: C, 53.25; H,3.46; N, 12.92%.

Preparation of Complex 2. Complex **2** was prepared in the same way as **1**, using [Mn(naphtmen)(H_2O)]ClO_4 (0.122 g, 0.2 mmol) instead of [Mn(salphen)(H_2O)]ClO_4 (0.0973 g, 0.2 mmol). Anal. Calcd for $C_{31}H_{29}Fe_{0.50}MnN_5O_4$(618.46): C, 60.20; H, 4.73; N, 11.32%. Found: C, 59.71; H, 4.88; N, 10.86%.

Preparation of Complex 3. The same procedure was used to prepare complex **3**, using [Mn(salen)(H_2O)]ClO_4 (0.0878 g, 0.2 mmol) instead of [Mn(salphen)(H_2O)]ClO_4 (0.0973 g, 0.2 mmol). Anal. Calcd for $C_{37}H_{30}FeMn_2N_{10}O_6$ (876.44): C, 50.71; H, 3.45; N, 15.98%. Found: C, 50.46; H, 3.27; N, 15.66%.

X-Ray Crystallography. Diffraction intensities for three complexes were collected on a computer-controlled Bruker SMART 1000 CCD diffractometer equipped with graphite-monochromated Mo Kα radiation with a radiation wavelength of 0.71073 Å, using the ω-scan technique. Lorentz polarization and absorption corrections were applied. The structures were solved by direct methods and refined with the full-matrix least-squares technique using the SHELXS-97 and SHELXL-97 programs.[30] Anisotropic thermal parameters were assigned to all nonhydrogen atoms. The hydrogen atoms were set in calculated positions and refined as riding atoms with a common fixed isotropic thermal parameter. Analytical expressions of neutral atom scattering factors were employed, and anomalous dispersion corrections were incorporated. Crystal data and details of structural determination refinement are summarized in Table 1.

Results and Discussion

Crystal structure of [Mn(salphen)(H_2O)]$_2$[Fe(CN)$_5$(NO)]·2CH_3OH (1). Complex **1** is composed of neutral trinuclear [Mn(salphen)(H_2O)]$_2$[Fe(CN)$_5$(NO)] units and CH_3OH molecules. A perspective view of the trinuclear [Mn(salphen)(H_2O)]$_2$[Fe(CN)$_5$(NO)] unit is shown in Figure 1, and selected bond lengths and angles are listed in Table 2.

In the trinuclear unit [Mn(salphen)(H_2O)]$_2$[Fe(CN)$_5$(NO)], the terminal Mn(III) ion is ligated by the Schiff base ligand salphen, one H_2O molecule, and a cyano bridge from the diamagnetic nitroprusside anion. The coordination sphere of Mn(III) is an axially elongated distorted octahedral environment; the bond distances in the axial position [Mn(1)−N(5) = 2.303 Å, Mn(1)−O(3) = 2.223 Å] are much longer than those in the equatorial plane (ranging from 1.856 to 1.987 Å). The comparison between the axial and the equatorial bond lengths clearly denotes the existence of the Jahn−Teller distortions in the octahedral Mn(III) ions. An $[Fe(CN)_5(NO)]^{2-}$ anion is sandwiched between a pair of [Mn(salphen)(H_2O)] fragments; the two CN^- groups in trans positions of the $[Fe(CN)_5(NO)]^{2-}$ moiety bridge two Mn(III) ions, resulting in the construction of a unique trinuclear [Mn(salphen)(H_2O)]$_2$[Fe(CN)$_5$(NO)]. The Fe atom of nitropusside occupies an inversion center, giving rise to a disorder of the nitrosyl group between two trans positions. The corresponding Fe−N/C distances (1.791 Å) are intermediate between the Fe−N and Fe−C distances typically observed in the $[Fe(CN)_5NO]^{2-}$ anion.[26a,31] The elongated axes associated with the two Mn(III) centers in the cyano-bridged cluster are rigorously parallel by virtue of their crystallographic inversion symmetry. The intramolecular separation between Mn(III) ions is 10.289 Å.

Figure 2 shows the packing diagram of trinuclear [Mn(salphen)(H_2O)]$_2$[Fe(CN)$_5$(NO)] units. All of the trinuclear units are packed along the same direction; the elongated axes of the Mn(III) ions are also arranged along one direction. Moreover, a hydrogen bond is found between the coordinated H_2O molecule (O3) and the

(27) Pfeifer, P.; Hesse, T.; Pfitzner, H.; Scholl, W.; Thielert, H. *J. Prakt. Chem.* **1937**, *149*, 217.
(28) Elwood, P. W. *Magnetochemistry*, Interscience: New York, 1956; p 78.
(29) Matsumoto, N.; Takemoto, N.; Ohyosi, A.; Ōkawa, H. *Bull. Chem. Soc. Jpn.* **1988**, *61*, 2984.
(30) (a) Sheldrick, G. M. *SHELXS-97*; Gottingen University: Gottingen, Germany, 1997. (b) Sheldrick, G. M. *SHELXL-97*; Gottingen University: Gottingen, Germany, 1997.
(31) Pressprich, M. R.; White, M. A.; Vekher, Y.; Coppens, P. *J. Am. Chem. Soc.* **1994**, *116*, 5233.

Table 1. Crystallographic Data and Structural Refinement for Complexes **1**−**3**

	1	**2**	**3**
empirical formula	$C_{47}H_{40}FeMn_2N_{10}O_9$	$C_{31}H_{29}Fe_{0.50}MnN_5O_4$	$C_{37}H_{30}FeMn_2N_{10}O_6$
fw	1054.62	618.46	876.44
cryst syst	triclinic	monoclinic	tetragonal
space group	$P\bar{1}$	$P2(1)/n$	$P4/ncc$
a (Å)	10.854(2)	10.861(2)	14.767(2)
b (Å)	11.239(2)	16.462(3)	14.767(2)
c (Å)	11.240(2)	16.068(3)	17.024(3)
α (deg)	101.51(3)	90	90
β (deg)	105.41(3)	103.94(3)	90
γ (deg)	114.93(3)	90	90
V (Å^3)	1119.8(4)	2788.2(10)	3712.1(11)
Z	1	4	4
ρ (Mg/m^3)	1.564	1.473	1.568
absorption coefficient	0.945 mm^{-1}	0.770 mm^{-1}	1.117 mm^{-1}
F(000)	540	1280	1784
cryst size (mm^3)	0.14 × 0.12 × 0.08	0.40 × 0.20 × 0.20	0.18 × 0.16 × 0.10
θ range for data collection	2.19 to 25.02°	3.11 to 25.10°	1.95 to 25.02°
reflns collected/unique	6360/3848 [R_{int} = 0.0648]	22580/4963 [R_{int} = 0.1030]	22781/1647 [R_{int} = 0.0356]
completeness to θ	97.2%	99.7%	99.6%
max and min transmission	0.9282 and 0.8791	0.8612 and 0.7482	0.8965 and 0.8243
Data/restraints/parameters	3848/9/323	4963/0/381	1647/24/137
goodness-of-fit on F^2	1.088	1.180	1.144
R_1 ($I > 2\sigma(I)$)	0.0702	0.0822	0.0536
wR_2 ($I > 2\sigma(I)$)	0.1872	0.1325	0.1421
R_1 (all data)	0.0810	0.1181	0.0544
wR_2 (all data)	0.1897	0.1441	0.1427

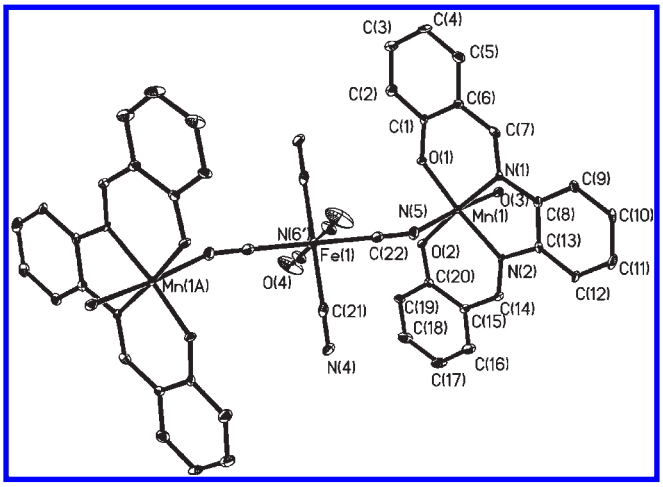

Figure 1. Perspective view of $[Mn(salphen)(H_2O)]_2[Fe(CN)_5(NO)]$ (**1**).

oxygen atom (O2) from the salphen ligand (O2···O3 = 2.789 Å). By this weak interaction, the O2···O3 bridge provides another superexchange approach between Mn(III) ions, resulting in a short intermolecular separation of 5.152 Å between Mn(III) ions.

Crystal Structure of $[Mn(naphtmen)(CH_3OH)]_2[Fe(CN)_5(NO)]$ (2). The structure of complex **2** consists of neutral trinuclear $[Mn(naphtmen)(CH_3OH)]_2[Fe(CN)_5(NO)]$ molecules. A perspective view of the trinuclear $[Mn(naphtmen)(CH_3OH)]_2[Fe(CN)_5(NO)]$ molecule is shown in Figure 3, and selected bond lengths and angles are listed in Table 3.

In the trinuclear molecule $[Mn(naphtmen)(CH_3OH)]_2[Fe(CN)_5(NO)]$, the terminal Mn(III) ion is coordinated to the Schiff base ligand naphtmen, one CH_3OH molecule, and a cyano bridge from the diamagnetic nitroprusside anion. The coordination sphere of Mn(III) is also an axially elongated distorted octahedral environment, the bond distances in the axial position [Mn(1)−N(4) = 2.287 Å, Mn(1)−O(4) = 2.357 Å] are significantly longer than those in the equatorial plane (ranging from 1.881 to 1.965 Å). Two $[Mn(naphtmen)(CH_3OH)]$ fragments are bridged by the diamagnetic nitroprusside anion, resulting in the formation of trinuclear molecule $[Mn(naphtmen)(CH_3OH)]_2[Fe(CN)_5(NO)]$. The intramolecular separation between Mn(III) ions is 10.370 Å.

Figure 4 shows the packing diagram of trinuclear $[Mn(naphtmen)(CH_3OH)]_2[Fe(CN)_5(NO)]$ molecules. Unlike complex **1**, the trinuclear molecules of complex **2** are packed along two directions, that is to say, there are two directions for the Jahn−Teller axes of the Mn(III) ions with an angle of ca. 120.5°. A hydrogen bond is found between the coordinated CH_3OH molecule (O4) and the nitrogen atom (N5) of the cyanide group from the nitroprusside anion (O4···N5 = 2.737 Å). The shortest intermolecular separation between Mn(III) ions is 8.396 Å.

Crystal Structure of $\{[Mn(salen)]_2[Fe(CN)_5(NO)]\cdot H_2O\}_n$ (3). The structure of complex **3** consists of two-dimensional framework $\{[Mn(salen)]_2[Fe(CN)_5(NO)]\}_n$ and H_2O molecules. In complex **3**, the coordination sphere of Mn(III) is still an axially elongated distorted octahedral environment; the bond distance in the axial position [Mn(1)−N(2) = 2.304 Å] is also longer than that in the equatorial plane [Mn(1)−O(2) = 1.888 Å, Mn(1)−N(4) = 1.987 Å]. The $[Fe(CN)_5(NO)]^{2-}$ anion coordinates to the axial site of the four $[Mn(salen)]^+$ entities through its four cyano nitrogen atoms, forming a two-dimensional network. The two-dimensional structure of $\{[Mn(salen)]_2[Fe(CN)_5(NO)]\cdot H_2O\}_n$ is shown in Figure 5, and selected bond lengths and angles are listed in Table 4. Similar to complex **2**, the elongated axes of the Mn(III) ions are also arranged along two directions with an angle of ca. 90°. The intramolecular separation between Mn(III) ions is 10.634 Å.

Table 2. Selected Bond Lengths (Å) and Angles (deg) for Complex **1**[a]

Mn(1)−O(1)	1.856(3)	Mn(1)−N(5)	2.303(5)
Mn(1)−O(2)	1.889(3)	Fe(1)−N(6′)#1	1.790(5)
Mn(1)−N(2)	1.986(4)	Fe(1)−C(23)	1.791(5)
Mn(1)−N(1)	1.987(4)	Fe(1)−C(22)	1.934(6)
Mn(1)−O(3)	2.223(4)	Fe(1)−C(21)	1.953(6)
O(1)−Mn(1)−O(2)	90.93(15)	N(6′)#1−Fe(1)−C(22)#1	89.1(2)
O(1)−Mn(1)−N(2)	174.68(15)	C(23)#1−Fe(1)−C(22)#1	89.1(2)
O(2)−Mn(1)−N(2)	93.36(15)	C(23)−Fe(1)−C(22)#1	90.9(2)
O(1)−Mn(1)−N(1)	93.50(15)	N(6′)#1−Fe(1)−C(22)	90.9(2)
O(2)−Mn(1)−N(1)	175.53(15)	C(23)#1−Fe(1)−C(22)	90.9(2)
N(2)−Mn(1)−N(1)	82.24(16)	C(23)−Fe(1)−C(22)	89.1(2)
O(1)−Mn(1)−O(3)	91.07(15)	C(22)#1−Fe(1)−C(22)	179.999(1)
O(2)−Mn(1)−O(3)	89.67(15)	N(6′)#1−Fe(1)−C(21)	89.4(2)
N(2)−Mn(1)−O(3)	85.81(15)	C(23)#1−Fe(1)−C(21)	89.4(2)
N(1)−Mn(1)−O(3)	90.79(16)	C(23)−Fe(1)−C(21)	90.6(2)
O(1)−Mn(1)−N(5)	92.24(16)	C(22)#1−Fe(1)−C(21)	89.5(2)
O(2)−Mn(1)−N(5)	88.66(16)	C(22)−Fe(1)−C(21)	90.5(2)
N(2)−Mn(1)−N(5)	91.01(16)	N(6′)#1−Fe(1)−C(21)#1	90.6(2)
N(1)−Mn(1)−N(5)	90.63(17)	C(23)#1−Fe(1)−C(21)#1	90.6(2)
O(3)−Mn(1)−N(5)	176.32(14)	C(23)−Fe(1)−C(21)#1	89.4(2)
N(6′)#1−Fe(1)−C(23)#1	0.0	C(22)#1−Fe(1)−C(21)#1	90.5(2)
N(6′)#1−Fe(1)−C(23)	180.0	C(22)−Fe(1)−C(21)#1	89.5(2)
C(23)#1−Fe(1)−C(23)	180.0	C(21)−Fe(1)−C(21)#1	179.998(2)

[a] Symmetry transformations used to generate equivalent atoms: #1 $-x+2, -y+1, -z+1$.

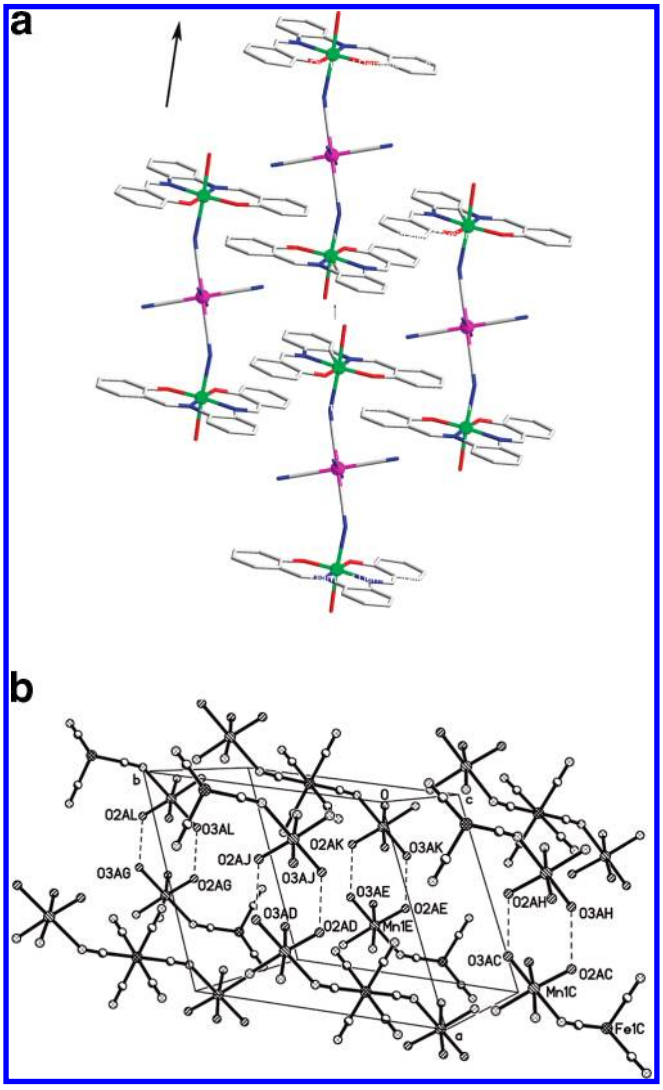

Figure 2. Packing diagram of trinuclear $[Mn(salphen)(H_2O)]_2[Fe(CN)_5(NO)]\cdot 2CH_3OH$ **1** units. (a) Green, Mn; pink, Fe. The arrow represents the elongated axis of the Mn(III) ion. (b) Hydrogen bonds between the coordinated H_2O molecule (O3) and the oxygen atom (O2) from the salphen ligand; the carbon atoms of the salphen ligand are omitted for clarity.

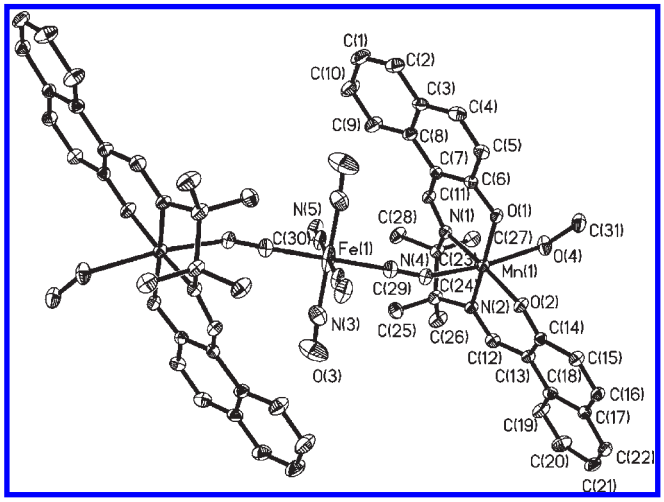

Figure 3. Perspective view of $[Mn(naphtmen)(CH_3OH)]_2[Fe(CN)_5(NO)]$ **2**.

IR Spectra. The IR spectra of these three complexes are very similar. The broad peaks at around 3300 cm^{-1} can be assigned to the vibration absorption of O−H from methanol or water molecules. Cyanide group stretching absorptions are found at ca. 2140 cm^{-1}, which are much less intense than in the $[Fe(CN)_5NO]^{2-}$ precursor, suggesting an important coordination effect of the cyano groups in the final compounds. The strong peak at ca. 1920 cm^{-1} is assigned to the N═O stretching vibration, which is lower than that found in the sodium salt (1940 cm^{-1}). Similar values have also been observed for other nitroprusside compounds such as $[Ni(bpy)_3][Fe(CN)_5NO]\cdot 3H_2O$ (1911 cm^{-1}).[32] The strong peaks appearing at 1630 and 1600 cm^{-1} may be attributed to the C═N bond stretching absorptions from the Schiff base ligands.

Variable-Temperature Magnetic Susceptibility Measurements. The magnetic susceptibility was measured in the temperature range 2−300 K on a Quantum Design MPMS-7 SQUID magnetometer in an applied magnetic

(32) Shyu, H. L.; Wei, H. H.; Wang, Y. *Inorg. Chim. Acta* **1997**, *258*, 81.

Table 3. Selected Bond Lengths (Å) and Angles (deg) for Complex **2**[a]

Mn(1)−O(1)	1.881(3)	Mn(1)−O(4)	2.357(3)
Mn(1)−O(2)	1.881(3)	Fe(1)−N(3)	1.809(6)
Mn(1)−N(2)	1.959(4)	Fe(1)−C(29)	1.920(5)
Mn(1)−N(1)	1.965(4)	Fe(1)−C(30)	1.925(5)
Mn(1)−N(4)	2.287(4)		
O(1)−Mn(1)−O(2)	96.64(13)	N(3)−Fe(1)−N(3)#1	180.0(4)
O(1)−Mn(1)−N(2)	168.95(15)	N(3)−Fe(1)−C(29)#1	92.3(2)
O(2)−Mn(1)−N(2)	91.21(14)	N(3)#1−Fe(1)−C(29)#1	87.7(2)
O(1)−Mn(1)−N(1)	91.04(14)	N(3)−Fe(1)−C(29)	87.7(2)
O(2)−Mn(1)−N(1)	172.08(15)	N(3)#1−Fe(1)−C(29)	92.3(2)
N(2)−Mn(1)−N(1)	80.92(15)	C(29)#1−Fe(1)−C(29)	180.0(2)
O(1)−Mn(1)−N(4)	85.50(14)	N(3)−Fe(1)−C(30)	90.2(2)
O(2)−Mn(1)−N(4)	93.54(14)	N(3)#1−Fe(1)−C(30)	89.8(2)
N(2)−Mn(1)−N(4)	101.82(15)	C(29)#1−Fe(1)−C(30)	90.16(19)
N(1)−Mn(1)−N(4)	88.99(15)	C(29)−Fe(1)−C(30)	89.84(19)
O(1)−Mn(1)−O(4)	83.77(12)	N(3)−Fe(1)−C(30)#1	89.8(2)
O(2)−Mn(1)−O(4)	85.45(13)	N(3)#1−Fe(1)−C(30)#1	90.2(2)
N(2)−Mn(1)−O(4)	89.13(14)	C(29)#1−Fe(1)−C(30)#1	89.84(19)
N(1)−Mn(1)−O(4)	93.47(14)	C(29)−Fe(1)−C(30)#1	90.16(19)
N(4)−Mn(1)−O(4)	169.03(13)	C(30)−Fe(1)−C(30)#1	180.0(3)

[a] Symmetry transformations used to generate equivalent atoms: #1 $-x+1, -y, -z$.

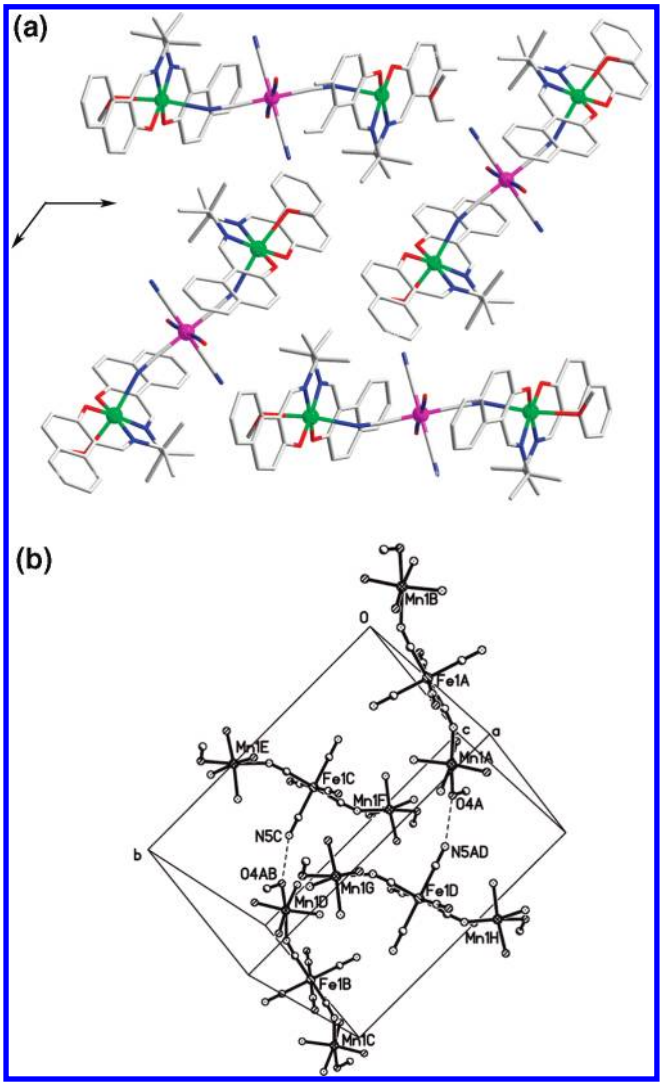

Figure 4. Packing diagram of trinuclear $[Mn(naphtmen)(CH_3OH)]_2$-$[Fe(CN)_5(NO)]$ (**2**) units. (a) Green, Mn; pink, Fe. The arrow represents the elongated axis of the Mn(III) ion. (b) Hydrogen bonds between the coordinated CH_3OH molecule (O4) and the nitrogen atom from the cyanide group (N5) from the nitroprusside anion. The carbon atoms of the naphtmen ligand are omitted for clarity.

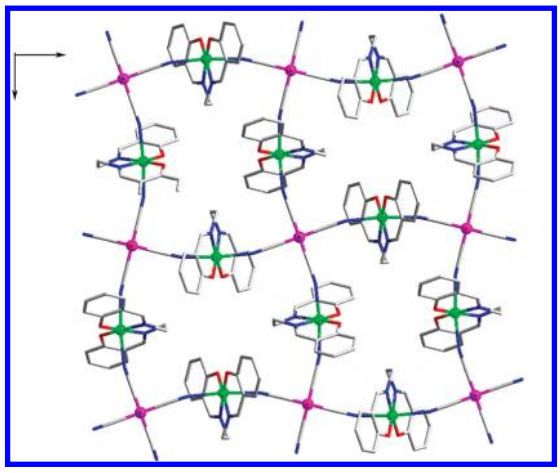

Figure 5. Two-dimensional structure of $\{[Mn(salen)]_2[Fe(CN)_5(NO)]\cdot H_2O\}_n$ (**3**). Green, Mn; purple, Fe. The arrow represents the elongated axis of the Mn(III) ion.

field of 2 KOe. As shown in Figure 6, for complex **1**, the room temperature value of $\chi_M T$ (6.01 cm^3 K mol^{-1}) is very close to that expected for two isolated Mn(III) ions ($\chi_M T$ = 6.0 cm^3 K mol^{-1} for g = 2.0, S = 2). Upon cooling, the $\chi_M T$ value slightly decreases from 300 to 50 K and then decreases sharply at low temperatures, reaching a value of 0.51 cm^3 K mol^{-1} at 2.0 K. Correspondingly, the χ_M versus T exhibits a maximum at ca. 7.0 K.

The sharp cusp in the χ_M versus T curve is usually assigned to the long-range 3D antiferromagnetic ordering. For complex **1**, long-range magnetic transition may not exist, as confirmed by the result that no sharp λ anomaly is found between 2 and 20 K in specific heat. Hence, the cusp in χ_M versus T at 7.0 K for complex **1** may result from the combination of zero-field splitting of Mn(III) ions and antiferromagnetic interaction between Mn(III) ions. All simulations with the experimental data without J or D failed. Taking into account both effects in the Hamiltonian given in eq 1 and using the computational program MAGPACK,[33] we have obtained an excellent simulation of the experimental data from the following parameters: $D = -2.46\ cm^{-1}$, $J = -0.45\ cm^{-1}$, and g = 2.02, where $\hat{S}_{iz}$ is the z component of the $\hat{S}_i$ operator, J is the magnetic coupling constant between two Mn(III) ions, D is the zero-field splitting parameter, and g is the Landé factor of the Mn(III) ion. The obtained J and D parameters are compatible with previously reported values in a similar complex.[26a]

$$\hat{H} = -2J\hat{S}_1\hat{S}_2 + D\sum_{i=1,2}\hat{S}_{iz}^2 + g\mu_B H\sum_{i=1,2}\hat{S}_i \qquad (1)$$

For complex **2**, the room temperature value for $\chi_M T$ (6.28 cm^3 K mol^{-1}) is a little larger than that expected for two isolated Mn(III) ions ($\chi_M T$ = 6.0 cm^3 K mol^{-1} for g = 2.0, S = 2). Upon cooling, there is a decrease in $\chi_M T$ similar to that found in complex **1**, but not so remarkable; the $\chi_M T$ value at 2.0 K (3.62 cm^3 K mol^{-1}) is also larger than that of complex **1** (0.51 cm^3 K mol^{-1}). Thus, while

(33) (a) Borrás-Almenar, J. J.; Clemente-Juan, J. M.; Coronado, E.; Tsukerblat, B. S. *Inorg. Chem.* **1999**, *38*, 6081. (b) Borrás-Almenar, J. J.; Clemente-Juan, J. M.; Coronado, E.; Tsukerblat, B. S. *J. Comput. Chem.* **2001**, *22*, 985.

Table 4. Selected Bond Lengths (Å) and Angles (deg) for Complex **3**[a]

Mn(1)−O(2)	1.888(3)	Fe(1)−N(3)	1.657(7)
Mn(1)−N(4)	1.987(4)	Fe(1)−C(1)	1.927(9)
Mn(1)−N(2)	2.304(4)	Fe(1)−C(2)	1.938(4)
O(2)−Mn(1)−O(2)#1	96.73(17)	N(2)#1−Mn(1)−N(2)	174.28(19)
O(2)−Mn(1)−N(4)	91.01(13)	N(3)−Fe(1)−C(1)	180.000(1)
O(2)#1−Mn(1)−N(4)	172.25(13)	N(3)−Fe(1)−C(2)#2	95.07(12)
N(4)−Mn(1)−N(4)#1	81.2(2)	N(3)−Fe(1)−C(2)	95.07(12)
O(2)−Mn(1)−N(2)#1	90.03(13)	C(1)−Fe(1)−C(2)	84.93(12)
O(2)#1−Mn(1)−N(2)#1	93.77(13)	C(2)#2−Fe(1)−C(2)	89.55(2)
N(4)−Mn(1)−N(2)#1	85.98(14)	C(2)#3−Fe(1)−C(2)	169.9(2)
O(2)−Mn(1)−N(2)	93.78(13)	C(2)#2−Fe(1)−C(2)#4	169.9(2)
N(4)−Mn(1)−N(2)	89.67(15)	C(2)−Fe(1)−C(2)#4	89.55(2)

[a] Symmetry transformations used to generate equivalent atoms: #1 $y + 1/2, x - 1/2, -z + 1/2$; #2 $-y + 1/2, x, z$; #3 $-x + 1/2, -y + 1/2, z$; #4 $y, -x + 1/2, z$.

complex **1** shows a maximum at 7.0 K, the susceptibility of complex **2** increases continuously down to 2 K. Taking into account both the zero-field splitting of Mn(III) ions and the antiferromagnetic interaction between Mn(III) ions and using the computational program MAGPACK,[33] an excellent simulation of the experimental data is obtained from the following parameters: $D = -0.40$ cm^{-1}, $J = -0.15$ cm^{-1}, and $g = 2.05$.

The room temperature value for $\chi_M T$ (3.06 cm^3 K mol^{-1}) of complex **3** is also very close to that expected for one isolated Mn(III) ion ($\chi_M T = 3.0$ cm^3 K mol^{-1} for $g = 2.0$, $S = 2$). Upon cooling, the $\chi_M T$ value decreases slightly from 300 to 50 K and then decreases sharply at low temperatures, reaching a value of 1.86 cm^3 K mol^{-1} at 2.0 K.

From the shapes of the $\chi_M T$ versus T curves for complex **3**, it is apparent that any intramolecular antiferromagnetic coupling is small as compared to the magnitude of the zero-field splitting (i.e., $D \gg J$). In order to analyze the experimental data, we tried to fit the data using a one-ion approximation model for Mn(III) ions, taking into account zero-field splitting by parameter D, and treating the exchange interaction between Mn(III) ions in the molecular field approximation (zj') as a perturbation, as in the zero-field Hamiltonian given in eq 2:

$$\check{H} = \hat{S} \cdot D \cdot \hat{S} - zj' \langle \hat{S}_Z \rangle \hat{S}_Z \qquad (2)$$

The resulting magnetic susceptibility equation is

$$\chi_M = \frac{2\chi_\perp + \chi_\parallel}{3}, x = D/KT$$

$$\chi_\perp = \frac{Ng^2\beta^2}{KT} \left\{ \frac{(6/x)[1 - \exp(-x)] + (4/3x)[\exp(-x) - \exp(-4x)]}{1 + 2\exp(-x) + 2\exp(-4x)} \right\}$$

$$\chi_\parallel = \frac{2Ng^2\beta^2}{KT} \left\{ \frac{\exp(-x) + 4\exp(-4x)}{1 + 2\exp(-x) + 2\exp(-4x)} \right\}$$

$$\chi_M' = \frac{\chi_M}{1 - (2zj'/Ng^2\beta^2)\chi_M}$$

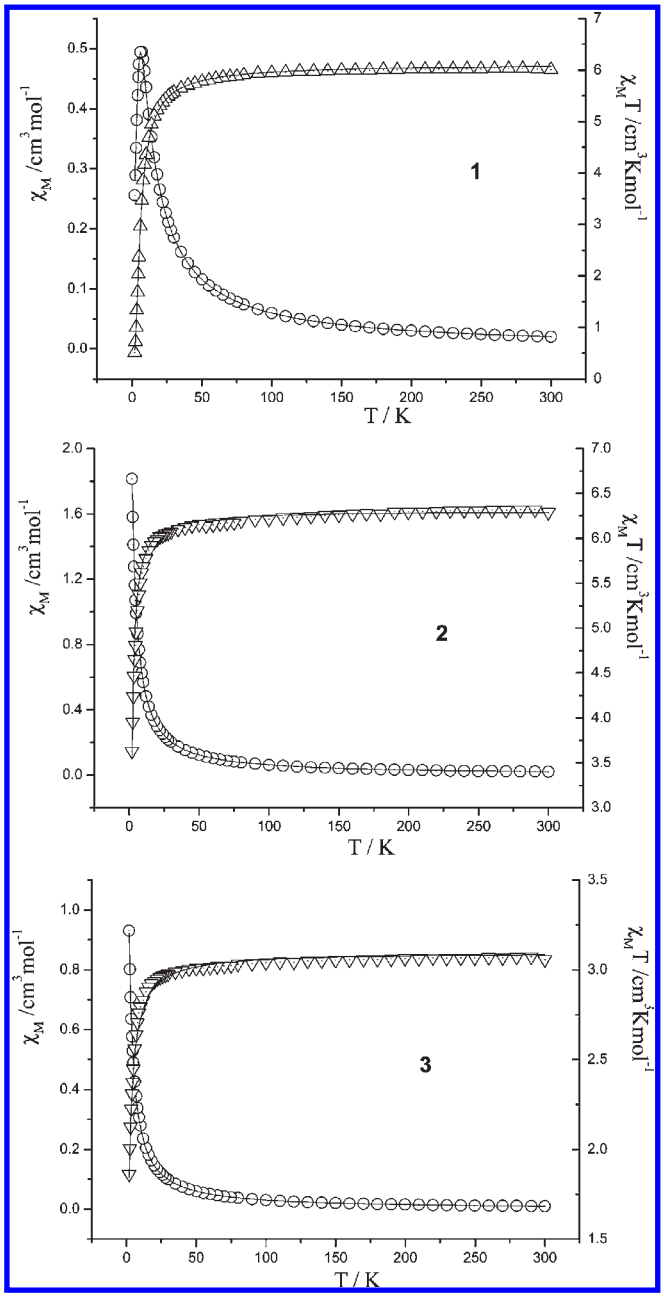

Figure 6. Experimental and calculated variations of χ_M (O) and $\chi_M T$ (Δ) versus T for complexes **1**−**3**.

This method has been used to fit chains of $Ru_2(V)$ units[34] and Cr(III) complexes[35] successfully. The best fitting for the experimental data gives $zJ' = -0.23$ cm^{-1}, $g = 2.03$, and $D = -0.43$ cm^{-1}. The agreement factor $R = \sum(\chi_{obsd} - \chi_{calcd})^2/\sum\chi_{obsd}^2$ is 8.98×10^{-5}.

The antiferromagnetic interaction of complex **1** is stronger than that in complex **2**. In complex **1**, there are at least two kinds of magnetic interactions, namely, (i) Mn(III)−Mn(III) through a diamagnetic nitroprusside anion bridge and (ii) Mn(III)−Mn(III) through an O2···O3 hydrogen bond bridge, as shown in Scheme 3.

(34) (a) Angaridis, P.; Berry, J. F.; Cotton, F. A.; Murillo, C. A.; Wang, X. *J. Am. Chem. Soc.* **2003**, *125*, 10327. (b) Colacio, E.; Lloret, F.; Kivekäs, R.; Suárez-Varela, J.; Sundberg, M. R.; Uggla, R. *Inorg. Chem.* **2003**, *42*, 560.

(35) Muñoz, M. C.; Julve, M.; Lloret, F.; Faus, J.; Andruh, M. *J. Chem. Soc., Dalton Trans.* **1998**, 3125.

Scheme 3. Magnetic Interactions in Complexes **1** and **2**

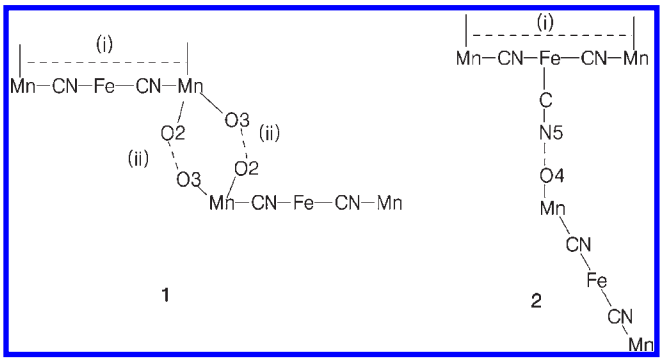

From the O2···O3 hydrogen bond, a short intermolecular separation of 5.152 Å between Mn(III) ions is formed. Considering that the long intramolecular separation between Mn(III) ions is 10.289 Å and the antiferromagnetic interaction between the Mn(III) ions through the diamagnetic nitroprusside anion is very weak, the O2···O3 hydrogen bond bridge may be the dominant superexchange approach.[17e] For complex **2**, the lack of component ii resulted in a weaker antiferromagnetic interaction of -0.15 cm^{-1}.

In six-coordinated manganese(III) complexes of Schiff bases, the anisotropic axis and available coordination sites are directed out of the plane of the partially blocking tetradentate ligands of the Schiff base. Owing to the structural distortion of the Mn(III) octahedral geometry, single-ion anisotropy likely plays an important role in the overall magnetic properties. Since the susceptibility measurement is a macroscopical and holistic measurement, the packing fashion may also affect the final magnetic behavior. The crystal packing of complex **1** (seen in Figure 2) indicates that the single-ion anisotropy is preserved and reinforced because the Jahn−Teller axes of Mn(III) ions are packing along the same direction. Whereas, in complex **2** or **3** (seen in Figures 4 and 5), the single-ion anisotropy is weakened and counteracted because the elongated axes of Mn(III) ions are not packing along the same direction. As a result, the phenomenological zero-field splitting parameter (D) in complex **2** or **3** is much smaller than that in complex **1**, although the coordination environment of the Mn(III) ion in complex **1** is similar to that of complexes **2** and **3**. As evidence, the crystal packing of complex $[Mn(3\text{-}MeOsalen)(H_2O)]_2[Fe(CN)_5NO]$ is the same as that of **1**, and its zero-field splitting parameter D is also close to that of complex **1**.[26a]

Variable-Field Magnetization Experiments of Complexes 2 and 3. The isothermal magnetizations, $M(H)$, of complexes **2** and **3** were measured at 2 K up to 50 kOe (Figure S1, Supporting Information). The increase of the magnetization M upon increasing the field reaches ca. 6.51 μ_B for complex **2** and 3.10 μ_B for complex **3** at 50 kOe, both lower than that of the Brillouin values expected for an $S = 4$ system for complex **2** (Mn^{III}_2 unit) and $S = 2$ for complex **3** (Mn^{III} unit), indicating that saturation has not yet been reached. This may be attributed to the antiferromagnetic interactions between Mn(III) ions and the zero-field splitting of Mn(III) ions.[36]

(36) Kennedy, B. J.; Murray, K. S. *Inorg. Chem.* **1985**, *24*, 1552.

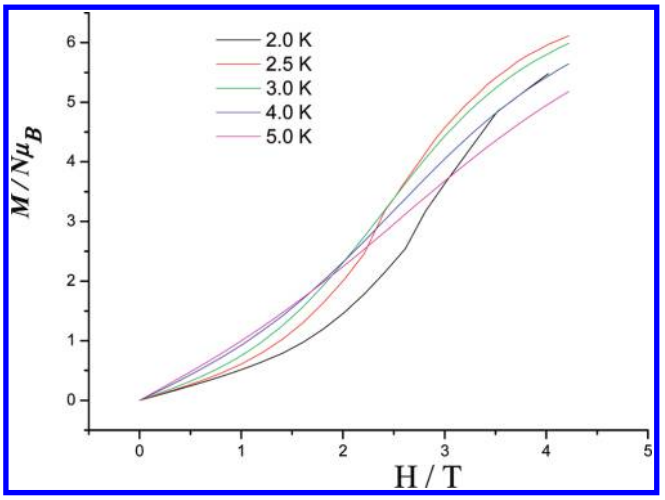

Figure 7. Variable-field magnetization experiments of complex **1** at different temperatures.

Spin-Flop Phenomenon of Complex 1. The field dependence of the magnetization for complex **1** at different temperatures (Figure 7) shows a pronounced sigmoidial shape, especially at lower temperatures below 5 K. The magnetization increases very slowly with increasing field due to considerably antiferromagnetic interactions between Mn(III) ions and zero-field splitting of Mn(III) ions and then increases rapidly, showing a spin-flop transition at a critical field of ca. 20 kOe. When the temperature reaches 5 K, the curve of magnetization versus the field is close to a straight line, indicative of a paramagnetic state. At higher fields, M reaches only ca. 6.0 $N\mu_B$ at 50 kOe, far from the expected saturated value of 8.0 $N\mu_B$ for two Mn(III) ions.

The temperature dependence of *ac* magnetic susceptibility presented in Figure 8 shows that the real part of *ac* magnetic susceptibility (χ') has a very broad peak at ca. 6.5 K under $H_{ac} = 3.5$ Oe and frequencies of 1, 10, and 100 Hz, and the out-of-phase *ac* magnetic susceptibility (χ'') is negligibly small. The maximum in $\chi'(T)$ arises as a result of short-range ordering, while the actual 3D magnetic ordering temperature lies at lower temperatures. There is no obvious frequency dependence in the $\chi_{ac}(T)$ response, which precludes any spin-glass[37] or SMM[7] behavior. The field dependence of *ac* magnetic susceptibility measured at 2.0 K shows a sharp peak in the real part at ca. 20 kOe, also suggesting the existence of a field-induced spin-flop transition. The position of the critical field is also in accordance with the inflection point in $M(H)$.

For complex **1**, the combination of a moderately strong zero-field splitting in Mn(III) ions and an appropriate antiferromagnetic interaction between the Mn(III) ions results in a typical spin-flop phenomenon. At 2 K, the spins of Mn(III) ions favor a preferred antiparallel alignment relative to the easy axis of magnetization. When the external field is of moderate intensity, the magnetization process proceeds through the spin-flop connected with reorientation of the antiferromagnetically coupled spins to the configuration perpendicular to the field, giving rise

(37) (a) Mydosh, J. A. *Spin Glasses: An Experimental Introduction*; Taylor and Francis: London, 1993. (b) Zheng, Y. Z.; Tong, M. L.; Zhang, W. X.; Chen, X. M. *Angew. Chem., Int. Ed.* **2006**, *45*, 6310.

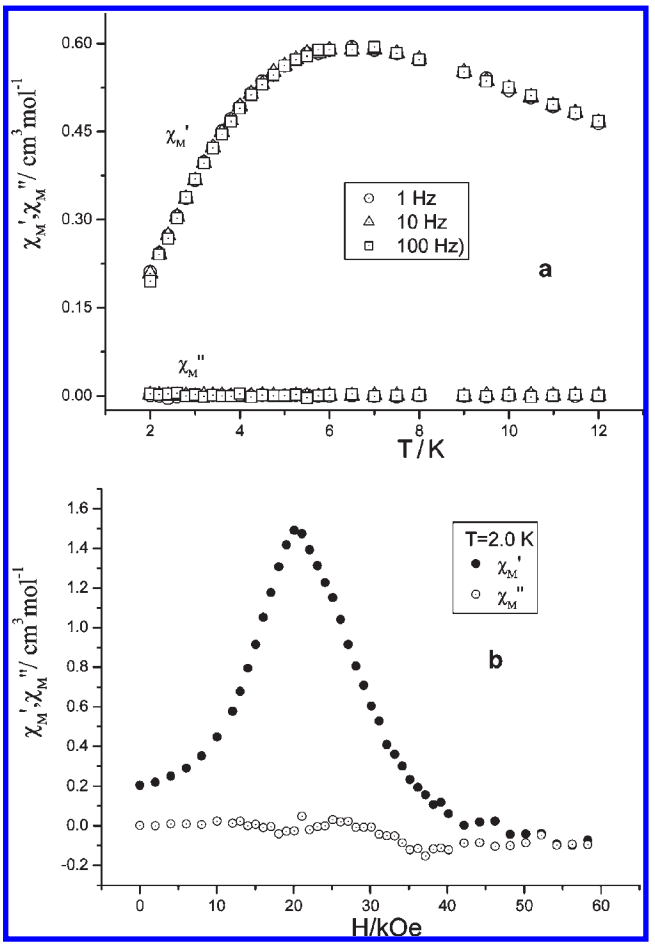

Figure 8. (a) The temperature dependence of ac magnetic susceptibility for complex **1**. (b) The field dependence of the ac magnetic susceptibility measurement at 2.0 K for complex **1**.

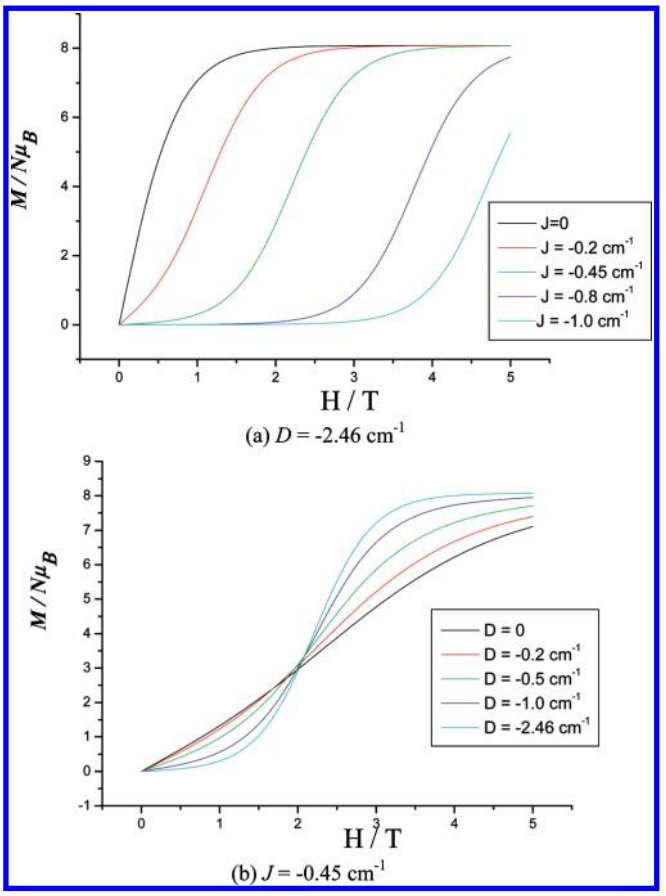

Figure 9. Simulation for the field dependence of the magnetization for a $Mn(III)_2$ system at 2 K.

to a field-induced spin-flop transition. Upon further increasing the H, the sublattice moments gradually rotate until another critical field, H_C, is reached, beyond which the average spin direction is parallel to the easy axis. These results suggest that the weak interactions between Mn(III) ions are finally overcome by increasing magnetic field. A similar spin-flop transition is also revealed in the cyanide-bridged tetrameric $W^{V}Mn^{III}_3$ assembly.[17d] In order to get more insight into the magnetic behavior of **1**, it might be necessary to further inspect the system as a single crystal.

Simulation for the Field Dependence of the Magnetization at 2 K. It is found that spin-flop behavior often occurs in some antiferromagnets with weak magnetic anisotropy.[15,38] For complex **1**, a long-range magnetic transition may not exist, so the spin-flop behavior can only be interpreted by the combination of zero-field splitting in Mn(III) ions and antiferromagnetic interaction between the Mn(III) ions. The pronounced sigmoidal shape of the $M(H)$ dependence at low temperatures is a characteristic behavior for spin-flop systems. A simulation of the binuclear $S = 4/2$ system for the field dependence of the magnetization at 2 K indicates that the spin-flop behavior is influenced by both the D and J parameters; moderate D and J parameters are needed for spin-flop behavior (Figure 9). If either of them is very small (for example, $J = -0.2\ cm^{-1}$ and $D = -2.46\ cm^{-1}$ or $J = -0.45\ cm^{-1}$ and $D = -0.20\ cm^{-1}$), no obvious spin-flop behavior is found. If the antiferromagnetic interactions are stronger, spin-flop behavior needs a much higher magnetic field. For the binuclear $S = 4/2$ system, if J is more negative than $-1.0\ cm^{-1}$, the spin-flop behavior needs a field larger than 5 T.

Specific Heat Study. The specific heat of complex **1** was measured in the temperature range 2−20 K on a Quantum Design PPMS-9 system (Figure S2, Supporting Information). The specific heat increases steadily with the temperature, and no sharp λ anomaly is found between 2 and 20 K, which indicates no long-range magnetic transition in complex **1**. Moreover, a broad hump below 7 K when Cp/T is plotted versus T suggests possible low-dimensional effects or short-range magnetic ordering.[39]

Conclusion

In this report, three bimetallic materials, $[Mn(salphen)(H_2O)]_2[Fe(CN)_5(NO)]\cdot 2CH_3OH$ (**1**), $[Mn(naphtmen)(CH_3OH)]_2[Fe(CN)_5(NO)]$ (**2**), and $\{[Mn(salen)]_2[Fe(CN)_5(NO)]\cdot H_2O\}_n$ (**3**), have been synthesized on the basis of $[Fe(CN)_5NO]^{2-}$ and $[Mn(SB)]^{+}$ building blocks (SB = salphen for **1**,

(38) Carlin, R. L.; Van-Duyneveldt, A. J. *Magnetic Properties of Transition Metal Compounds*; Springer-Verlag: New York, 1977.

(39) De Jongh, L. J. *Magnetic Properties of Layered Transition Metal Compounds*; Kluwer Academic Publishers: Dordrecht, The Netherlands, 1990.

naphtmen for **2**, and salen for **3**). The structural analyses show that complexes **1** and **2** consist of the discrete linear trinuclear $[Mn(SB)]_2[Fe(CN)_5(NO)]$ units; in complex **3**, the nitroprusside anion coordinates to the axial site of the four $[Mn(salen)]^+$ entities through its four cyano nitrogen atoms, forming a two-dimensional network. The magnetic analysis indicates that the nitroprusside bridging ligand propagates a very weak antiferromagnetic exchange, and significant couplings are transmitted through the hydrogen bonds in complex **1**. Single-ion anisotropy plays an important role in the overall magnetic properties. For complex **1**, the elongated axes of Mn(III) ions are packing along the same direction, which leads to a relatively larger value of $D = -2.46\ cm^{-1}$. The combination of a moderate zero-field splitting in Mn(III) ions and an appropriate antiferromagnetic interaction between the Mn(III) ions results in a typical spin-flop transition with a critical field of 20 kOe. Whereas, in complexes **2** and **3**, the single-ion anisotropy is weakened and counteracted because the elongated axes of Mn(III) ions are not packing along the same direction. As a result, no more interesting phenomena in magnetism are found except weak antiferromagnteic interaction.

Acknowledgment. This project was granted financial support from the National Natural Science Foundation of China (Nos. 20601014, 20631030, and 90922032), National Basic Research Program of China (973 Program, 2007CB815305), and Natural Science Foundation of Tianjin (09JCYBJC05500).

Note Added after ASAP Publication: This paper was published on January 12, 2010, containing the same data as those referenced in ref 26b. Therefore, some of the original wording in the Abstract and Conclusion sections has been changed to match this reference. This correct version was reposted on February 8, 2010.

Supporting Information Available: Variable-field magnetization experiments of complexes **2** and **3** at 2 K (Figure S1). Temperature dependence of the heat capacity *Cp* (O) and after normalization with temperature (Cp/T, Δ) for complex **1** (Figure S2). X-ray crystallographic files, in CIF format, for complexes $[Mn(salphen)(H_2O)]_2[Fe(CN)_5(NO)]\cdot 2CH_3OH$ (**1**), $[Mn(naphtmen)(CH_3OH)]_2[Fe(CN)_5(NO)]$ (**2**), and $\{[Mn(salen)]_2[Fe(CN)_5(NO)]\cdot H_2O\}_n$ (**3**). This material is available free of charge via the Internet at http://pubs.acs.org.